

## Original Article

# Effects of silencing p27RF-Rho expression on the biological behavior of A549 human non-small cell lung cancer cells

Zongzhe Xuan, Hongfei Cai, Caiwen Chen, Youbin Cui

Department of Thoracic Surgery, The First Hospital of Jilin University, Changchun 130021, China

Received September 27, 2017; Accepted January 23, 2018; Epub May 15, 2018; Published May 30, 2018

**Abstract:** *Background and aim:* We explored the feasibility of p27RF-Rho silencing as a targeted therapy for lung cancer. To this end, p27RF-Rho was silenced in A549 NSCLC cells followed by assessment of the associated effects on cell proliferation, cell cycle, apoptosis, migration, and invasion. *Methods* A p27RF-Rho RNAi lentivirus was constructed followed by infection of A549 cells, which were divided into a p27RF-Rho-siRNA group, a scrambled siRNA negative control group, and a A549 blank control group. Western blotting was used to assess the expression and successful silencing of p27RF-Rho. MTT assays were used to measure cell proliferation, qPCR was used to detect expression of p16 and CDK5, and Western blotting was used to evaluate expression of the cell cycle-related proteins p27<sup>Kip1</sup> and cyclin-E, as well as the expression of p53, Bax, and the antiapoptotic protein Bcl-2. Scratch tests were used to measure cell migration, and transwell assays were adopted to evaluate A549 cell invasion. *Results:* A lentiviral vector containing the p27RF-Rho interference sequence was successfully constructed and p27RF-Rho-siRNA stable cell lines were established. Western blotting confirmed that expression of p27RF-Rho was significantly decreased. The proliferation of cells in the experimental group was significantly lower than that in the scrambled siRNA negative control and blank control groups. Expression of p53 and Bax protein was significantly higher in the experimental group than in the scrambled siRNA negative control and blank control groups, whereas levels of Bcl-2 were decreased. The migratory and invasive abilities of cells in the experimental group were significantly reduced compared to the scrambled siRNA negative control and blank control groups. *Conclusions:* Silencing of p27RF-Rho can inhibit the proliferation, migration and invasion of A549 NSCLC cells and promote A549 NSCLC cell apoptosis. Thus, p27RF-Rho silencing may be useful as a targeted therapy for lung cancer.

**Keywords:** Non-small cell lung cancer, p27RF-Rho, gene silencing, A549 cells, targeted therapy

## Introduction

Lung cancer (LC) is one of the most common malignant tumors in the world, with an annually increasing incidence and mortality. Recent studies have demonstrated that LC accounts for 13% of all cancer cases and up to 18% of cancer-related deaths [1, 2]. In addition to the high morbidity and mortality, patients with LC have a poor prognosis and short median survival time. Most patients with LC are diagnosed in the middle and late stages when many tumors have metastasized. Even after diagnosis and immediate treatment, the median survival is often no more than 1 year, or even shorter [3]. Non-small cell lung cancer (NSCLC) accounts for 80-85% of all lung cancer cases; the three main types are adenocarcinoma,

squamous cell carcinoma (epidermoid style), and large cell carcinoma [4]. Adenocarcinoma is the most common type of LC and is the most common form in non-smokers [5]. Presently, the 5-year survival rate of NSCLC patients is even lower than 15% [6], which creates a serious threat to physical and mental health and also causes a great economic burden to the patient's family and the public health system. Current treatments for NSCLC such as surgery, chemotherapy and radiotherapy have been used for a long time, however 30-60% of NSCLC patients still die within 5 years of surgery [7, 8]. Therefore, with the recent development of precision medical techniques, it is particularly important to identify novel genes for targeted LC therapy.

# Effects of silencing p27RF-Rho expression on A549 cells

**Table 1.** Primer sequence of shRNA

Gene	Primer sequence
p27RF-Rho-shRNA	5'-GGAGCTGGTTGTACAGTTTCAAGAGAACTGTACAACCAGCTCCTTTTT-3'
	5'-AAAAAGGAGCTGGTTGTACAGTTTCTTGAACACTGTACAACCAGCTCCGTAC-3'
Scramble-shRNA	5'-GTTGCATACGTGCGGTGATATCAAGAGATATCACCGCACGTATGCAACTTTTT-3'
	5'-AAAAAGTTGCATACGTGCGGTGATATCTTGAATATCACCGCACGTATGCAACGTAC-3'

p27kip1-releasing factor from RhoA (p27RF-Rho) is a 161-amino acid protein that regulates the activity of Ras homolog (Rho) member GTPase, which functions as a molecular switch in a number of important cellular signal transduction pathways. Rho GTPase plays a key role in cell migration and is closely related to the migration and invasion ability of many tumors [9, 10]. The Rho GTPase family consists of three subfamilies: RAC, Cdc42, and Rho. RhoA, a member of the Rho subfamily, is overexpressed in a variety of malignancies including NSCLC, and plays a critical role in regulating tumor cell proliferation, apoptosis, differentiation, and angiogenesis [11]. Another family member, RhoC, is highly expressed in NSCLC and is associated with invasion and metastasis [12]. Recent studies have demonstrated that p27RF-Rho can act on RhoA and RhoC and their downstream molecules [13]. In addition, p27RF-Rho is associated with p27<sup>kip1</sup> protein, and can regulate the proliferation, migration, and invasion of hepatoma cells [14]. p27<sup>kip1</sup> is a cell cycle-associated protein that plays an important role in regulating the tumor cell cycle when expressed in the nucleus [15]. Conversely, when located in the cytoplasm it functions as a proto-oncogene and overexpression in the cytoplasm can affect tumor invasion and patient prognosis [16].

RNA interference (RNAi) is a highly specific method for silencing target genes that is widely used as an anti-tumor and anti-virus tool, as well as for the investigation of signal transduction pathways in cells. Lentivirus-mediated RNAi is the most commonly used method for RNAi delivery [17-19]. To study the biological function of p27RF-Rho in NSCLC, the current study silenced p27RF-Rho and investigated the associated effects on the proliferation, apoptosis, migration, and invasion of A549 cells, as well as the possible underlying molecular mechanisms.

## Materials and methods

### Materials

NSCLC A549 cells and 293T cells were obtained from the Chinese Academy of Sciences 4753

Shanghai Cell Bank (Shanghai, China). The eukaryotic U6-CMV-copGFP-PGK-Puro-p27RF-Rho-silencing and negative control U6-CMV-copGFP-PGK-Puro-Scrambled viral expression vectors were synthesized in our laboratory. *E. coli* DH5a competent cells were purchased from Invitrogen (Carlsbad, CA, USA).

### Methods

**Construction and extraction of the RNAi lentiviral vector: siRNA design and synthesis:** A siRNA interference sequence was designed to down-regulate the expression of *p27RF-Rho*. The shRNA primers were annealed to form double-stranded fragments with cohesive ends; the sequences are shown in **Table 1**. The reaction system included 2  $\mu$ L shRNA-F, 2  $\mu$ L shRNA-R, 2  $\mu$ L 10  $\times$  buffer and 14  $\mu$ L ddH<sub>2</sub>O. The reaction conditions were as follows: 95°C for 5 min, 72°C for 10 min, and room temperature for 1 h.

**Preparation of the expression vector: Enzymatic cleavage of the U6-CMV-copGFP-PGK-Puro lentivirus interference vector:** The vector was cleaved in a reaction containing 6  $\mu$ L 10  $\times$  buffer, 10  $\mu$ L lentivirus interference vector, 1  $\mu$ L *KpnI*, 1  $\mu$ L *HpaI*, and 42  $\mu$ L ddH<sub>2</sub>O. The components were mixed and then incubated at 37°C for 3 h.

**Ligation of fragments into the expression vector:** To construct the U6-shRNA-CMV-copGFP-PGK-Puro vector, 3  $\mu$ L annealing products, 3  $\mu$ L lentiviral vector fragments, 1  $\mu$ L T4 ligase, 2  $\mu$ L, 10  $\times$  T4 buffer, and 11  $\mu$ L ddH<sub>2</sub>O were mixed and incubated overnight at 16°C.

**Competent cell transformation:** Competent cells were removed from storage at -80°C and placed on ice for 10 min to thaw the bacteria. Then, 10  $\mu$ L of the ligation product obtained in the previous step was added to the competent bacteria and placed on ice for up to 30 min, followed by heat shock at 42°C for 90 s, and then immediate transfer to ice for 2 min. Next, 500  $\mu$ L SOC liquid culture medium was added and the cells were incubated at 37°C for 1 h. After

## Effects of silencing p27RF-Rho expression on A549 cells

centrifugation at 3,000 rpm at room temperature for 5 min, a pipette was used to remove most of the liquid culture, leaving about 150  $\mu$ L liquid medium in the tube. The broth was plated on LB solid medium containing the appropriate antibiotic to select the recombinant plasmid, after which the plates were incubated at 37°C overnight.

### *Extraction and identification of the plasmid:*

Five single colonies were selected using a sterile tip and added to culture tubes and 5 mL of LB-resistant liquid medium was added and the cells were incubated overnight at 37°C with stirring for 16-18 h. A total of 4 mL of bacterial culture was added to a centrifuge tube and centrifuged at 12,000 rpm for 1 min, after which the supernatant was discarded. Next, 250  $\mu$ L Buffer S1 from the Plasmid DNA Purification Kit containing RNaseA was added, the cells were pelleted, and the bacteria were resuspended in 250  $\mu$ L Buffer S2. The tube was quickly and gently inverted 4-6 times to mix and this step was not allowed to take longer than 5 min. Next, 350  $\mu$ L Buffer S3 was added, and the tube was inverted 4-6 times to mix well and centrifuged at 12,000 rpm at room temperature for 10 min. The supernatant was transferred to a new DNA adsorption column and centrifuged at 12,000 rpm at room temperature for 1 min, after which the waste was discarded. Then, 700  $\mu$ L wash solution was added to the column, the column was centrifuged at 12,000 rpm at room temperature for 1 min, the waste was discarded, and this step was repeated. After an additional centrifugation at 12,000 rpm for 1 min, the column was dried until the alcohol odor had disappeared. Then the DNA adsorption column was placed in a new centrifuge tube, and 60  $\mu$ L sterilized deionized water that had been preheated to 55°C was added. The chamber was allowed to stand at room temperature for 2 min and then centrifuged at 12,000 rpm for 2 min to extract the plasmid DNA.

*Lentivirus packaging and collection:* The vector plasmid and psPAX and pMD2G plasmid backbones were co-transfected into 293T cells for lentivirus packaging. 293T cells in the logarithmic growth phase were digested and a cell suspension was prepared. The cells were inoculated in cell culture plates at a density of  $2 \times 10^7$  cells in 20 mL and incubated overnight. The

cells were transfected when the cell density reached 80%. Briefly, 2  $\mu$ g expression plasmid, 1.5  $\mu$ g psPAX2, and 1.5  $\mu$ g pMD2G were added to 500  $\mu$ L serum-free medium. A total of 500  $\mu$ L serum-free medium and 15  $\mu$ L Lipofectamine 2000 were added to another tube and incubated at room temperature for 5 min. The contents of the two tubes were mixed and incubated at room temperature for 20 min. Then, the transfection mixture was added dropwise to the cell culture. After incubation for 4-6 h, the culture media was discarded and fresh normal medium containing 10% fetal bovine serum was added. After 24 h, the transfection efficiency was observed under a fluorescence microscope and typical transfection efficiencies were >70%. Culture supernatants were collected separately after 24 h and 72 h, centrifuged at 3,000 rpm for 20 min, and syringe-filtered using a 0.45  $\mu$ m filter. Cells were concentrated by centrifugation at 12,000 rpm, followed by storage at -80°C until subsequent use.

*Lentivirus-transfected A549 cells:* A549 cells were divided into three groups: the p27RF-Rho-siRNA experimental group, the scrambled siRNA negative control group, and the blank control group. The cells were harvested in the logarithmic growth phase. A cell suspension was prepared and cells were seeded into 6-well plates at a density of  $1.2 \times 10^6$  cells/well. After incubation for 24 h, the cells reached about 80% confluence. Cells in the experimental group were infected by adding 3  $\mu$ L p27RF-Rho-siRNA lentivirus, the control group was infected with 3  $\mu$ L scrambled siRNA and untreated cells were used as the blank control group. Puromycin was added to select stable cell lines for subsequent experiments.

*Western blotting:* Western blotting was used to detect the effects of transfection on p27RF-Rho (the silencing efficiency), p27<sup>KIP1</sup>, cyclin E, p53, Bax and Bcl-2 levels. Cultured cells were washed twice with PBS that had been pre-cooled. Then 400  $\mu$ L RIPA lysis buffer containing protease inhibitors was added and cells were incubated on ice for 30 min; tubes were shaken a few times during the lysis process to ensure that the lysis buffer made full contact with the cells. After centrifugation at 12,000 rpm at 4°C for 10 min, the supernatant was collected and the protein concentration was deter-

## Effects of silencing p27RF-Rho expression on A549 cells

**Table 2.** Primer sequences

Gene	Two-way primer sequences (5'-3')
p16	F: CACCGTCTTCAGGGCTTCTTGTTT R: CCCCTGAGCTTCCCTAGTTCACAA
CDK-5	F: CAGTTGCAATGGTGACCTCG R: CTGGCAGCTTGGTCATAGAGG
$\alpha$ -Tubulin	F: GTTACCAGGGCTGCCTTCTC R: GGGTTTCCCGTTGAT GACC

mined using the BCA Protein Assay Kit (Thermo Fisher, Waltham, MA, USA). Next, 30  $\mu$ g protein was mixed with 5  $\times$  bromophenol blue loading buffer at a ratio of 4:1, boiled in a water bath for 5 min, and resolved on 12% SDS-PAGE gels. After electrotransfer of proteins to PVDF membranes using the Bio-Rad Microelectronic Transfer System (Hercules, CA, USA), the membranes were washed three times with TBS containing 0.1% Tween (TBST) and incubated overnight with primary antibody at 4°C. After washing three times, the membranes were incubated with secondary antibody for 2 h and the signal was developed using ECL chemiluminescence reagent.

**Quantitative polymerase chain reaction:** The mRNA expression of p16 and cyclin-dependent kinase-5 (CDK5) was detected using quantitative polymerase chain reaction (qPCR). The primer sequences are shown in **Table 2**. The cells were collected and the culture media were discarded. Then the cells were washed three times with pre-cooled PBS and 1-2 mL Trizol was added to each 10 cm<sup>2</sup> of cultured cells. After mixing, chloroform was added and mixed to produce a milky white solution. After incubation for 5 min, the cells were centrifuged at 12,000 rpm for 15 min. The supernatant was removed and isopropanol was added. After gently mixing and incubation at room temperature for 10 min and centrifugation at 12,000 rpm at 4°C for 10 min, the supernatant was removed followed by a 75% ethanol wash, and centrifugation at 7,500 rpm at 4°C for 5 min. The washing was repeated once, and the supernatant was carefully removed. After drying the RNA at room temperature, the appropriate amount of RNase-free ddH<sub>2</sub>O was added to dissolve the pellet. The concentration was measured and the RNA was stored at -80°C. For PCR, 5  $\mu$ L RNA was added to 595  $\mu$ L 1  $\times$  TE buffer and the absorbance was measured at

260 nm and 280 nm. The RNA concentration was calculated using the formula  $OD_{260} \times \text{dilution factor} \times 0.04 \mu\text{g}/\mu\text{L}$  (cuvette diameter 1 cm). An  $OD_{260/280}$  of 1.8-2.1 was considered highly pure extracted RNA. The extracted RNA was analyzed and the qPCR data were analyzed using the 2<sup>- $\Delta\Delta$ CT</sup> method to determine target gene expression.

**MTT cell proliferation assay:** The MTT reagent was dissolved with 0.01 mol/L PBS into a concentration of 5 mg/mL and sterilized using a 0.22  $\mu$ m membrane filter, stored at -20°C in the dark, and used within 1 week. The three groups of cells transfected with lentivirus for 24 h were inoculated into 96-well plates at a density of 0.5  $\times$  10<sup>4</sup> cells/well. 20  $\mu$ L MTT was added to each well and the plates were cultured for another 4-6 h. The supernatant was aspirated using a pipette, 150  $\mu$ L DMSO was added to each well, and the plates were shaken for 10 min. The absorbance at 490 nm was measured using a Bio-Rad Multifunctional Microplate Reader, the results were recorded, and the mean values were obtained. Proliferation curves were calculated for each group.

**Scratch wound healing assay:** Before the cells were plated, a straight horizontal line was drawn on the back of a 96-well plate across each well using a marker with 3-5 lines drawn per well. The three groups of cells were transfected with lentivirus for 24 h, and cell suspensions were prepared and seeded into 96-well plates at a density of 4  $\times$  10<sup>4</sup> cells/well. When the cells were almost confluent, a scratch was made on the bottom of the well. The cells were washed three times with PBS to remove cell debris, and the media was replaced with serum-free medium. Then the plates were incubated and photographed at 0 and 24 h. ImageJ software was used to calculate the distance between horizontal lines from 6-8 random fields and to calculate the mean.

**Transwell cell invasion assays:** To prepare the Transwell chambers, Matrigel matrix was pre-mixed overnight at 4°C and then diluted 1:8 in serum-free DMEM medium. After fully mixing, a pipette gun head that had been pre-cooled to 4°C was used to absorb 1000  $\mu$ L of the mixture to the bottom of the upper chamber with gentle shaking to ensure an even distribution and avoid bubbles. The chamber was placed in an

## Effects of silencing p27RF-Rho expression on A549 cells

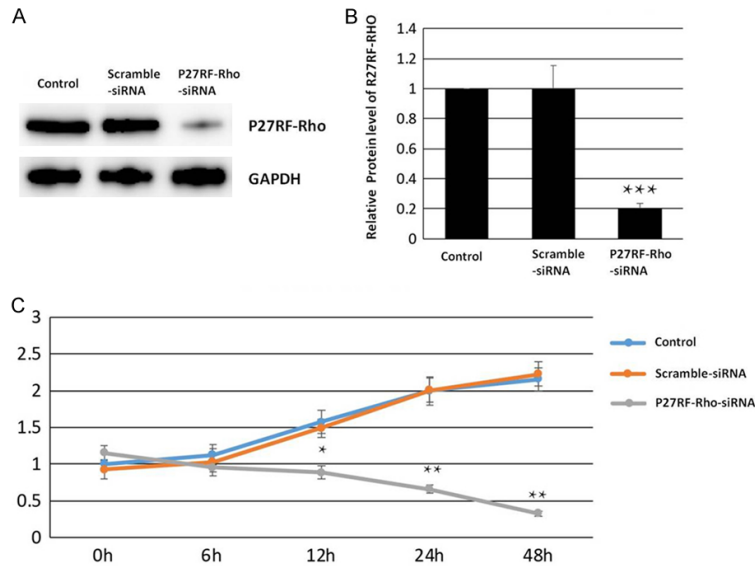


**Figure 1.** Silencing efficiency of p27RF-Rho siRNA. Expression was significantly lower in the p27RF-Rho group ( $P < 0.05$ ) and expression was reduced (A, B). A549 cell growth curves in different groups. Cell viability was significantly decreased when p27RF-Rho was silenced compared to the scrambled siRNA negative control group and the blank control groups ( $P < 0.05$ ) (C).

orifice plate and incubated at 37°C with 5% CO<sub>2</sub>. After 4 h, the matrix was solidified and removed. After removing the chamber, the moisture was aspirated from the Matrigel and 500 μL serum-free DMEM was added to the lower chamber to hydrate the basement membrane. The three groups of cells were cultured in serum-free medium for 12-16 h, and the media was discarded. Then the cells were washed 1-2 times with PBS, digested with trypsin-EDTA, and counted. The cell density was adjusted to 2000 cells/well in serum-free medium containing 0.1% BSA. A total of 500 μL complete medium was added to the 24-well plate and  $2 \times 10^5$  cells/well were seeded in a transwell chamber that had been coated with Matrigel. The 24-well plates were gently placed in an incubator and cultured for 16-24 h. After incubation, the culture media was removed from the upper chamber and the cells were carefully wiped using a cotton swab. The bottom of the chamber was fixed in 4% paraformaldehyde for 30 min, washed with PBS, stained with 0.1% crystal violet for 30 min, and washed with PBS 1-2 times. The cells were placed on a slide and observed and counted using an inverted microscope. Five fields were randomly selected and the number of cells per milliliter was calculated. The mean was cal-

culated and the groups were compared statistically.

### Statistical analysis

SPSS version 18.0 software was used to analyze the data. Measurement data are presented as the mean  $\pm$  standard deviations ( $\bar{X} \pm S$ ) and comparisons between two groups were made using *t*-tests.  $P < 0.05$  was used to define statistical significance.

## Results

### p27RF-Rho silencing efficiency

The relative expression of p27RF-Rho protein in the p27RF-Rho interference group was  $0.201 \pm 0.052$ , compared to  $0.99 \pm 0.035$  in the scrambled siRNA negative control group and  $1 \pm 0.093$  in the blank control group. The expression was significantly lower in the p27RF-Rho group ( $P < 0.05$ ), and expression was reduced by  $79.8 \pm 2.37\%$  (Figure 1A and 1B).

### Silencing of p27RF-Rho inhibits A549 cell proliferation

The results of the MTT assay showed that there were no significant differences in cell growth among the three groups. However, after 12 h of culture, cell viability was significantly decreased when p27RF-Rho was silenced compared to the scrambled siRNA negative control group and the blank control groups ( $P < 0.05$ ). As the culture time increased, the inhibitory effects of p27RF-Rho interference on cell proliferation became more obvious (Figure 1C).

### Silencing of p27RF-Rho affects the expression of cell cycle-associated genes and proteins in A549 cells

The mRNA expression of *p16* was significantly higher in the p27RF-Rho group than in the scrambled siRNA negative control and the blank control groups ( $P < 0.001$ ) whereas *CDK5* expression was significantly decreased ( $P < 0.01$ ) (Figure 2A and 2B). Western blotting

## Effects of silencing p27RF-Rho expression on A549 cells

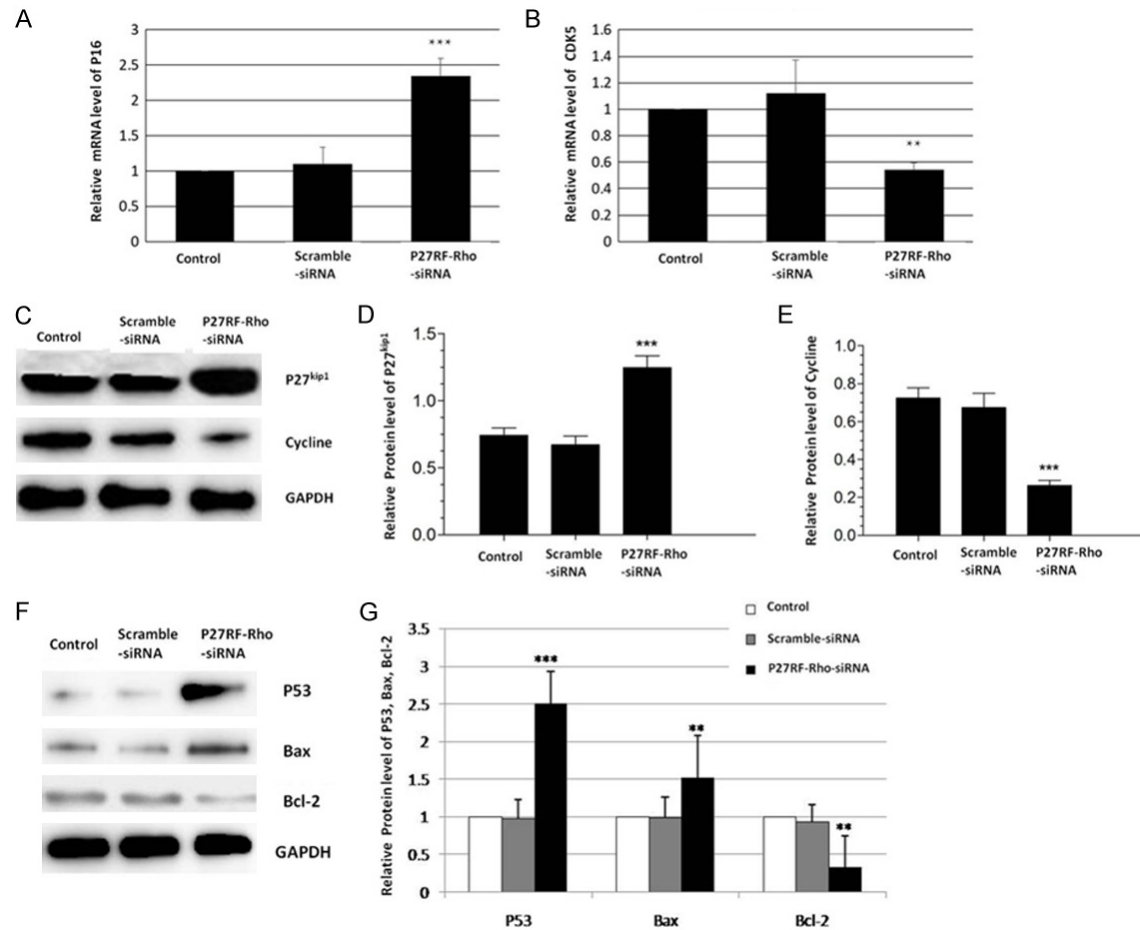


**Figure 2.** The expression of genes and proteins related to the cell cycle and apoptosis. The mRNA expression of *p16* was significantly higher in the p27RF-Rho group than in the negative control and the blank control groups ( $P < 0.001$ ) whereas CDK5 expression was significantly decreased ( $P < 0.01$ ) (A, B). Expression of p27<sup>kip1</sup> was significantly higher ( $P < 0.001$ ) and cyclin E levels were significantly lower in the p27RF-Rho group compared to the scramble siRNA negative control and blank control groups ( $P < 0.001$ ) (C, D, E). Silencing p27RF-Rho promotes A549 cell apoptosis. The expression of p53 and Bax was significantly higher in p27RF-Rho-treated cells compared to the negative control and blank control groups ( $P < 0.01$ ). In addition, expression of the anti-apoptotic protein Bcl-2 was decreased in the p27RF-Rho interference group (F, G).

revealed that expression of p27<sup>kip1</sup> was significantly higher ( $P < 0.001$ ) and cyclin E levels were significantly lower in the p27RF-Rho group compared to the scramble siRNA negative control and blank control groups ( $P < 0.001$ ) (Figure 2C-E).

### Silencing p27RF-Rho promotes A549 cell apoptosis

Western blotting showed that the expression of p53 and Bax was significantly higher in p27RF-Rho-treated cells compared to the scrambled siRNA negative control and the blank control groups ( $P < 0.01$ ). In addition, expression of the

anti-apoptotic protein Bcl-2 was decreased in the p27RF-Rho interference group (Figure 2E and 2F).

### Silencing of p27RF-Rho inhibits A549 cell migration

The results of the scratch test showed that after 24 h of culture, most of the scratches in the p27RF-Rho interference group had no cell coverage, whereas cells in the scramble siRNA negative control and blank control groups covered most of the scratch area. Therefore, silencing of p27RF-Rho significantly inhibited A549 cell migration ( $P < 0.05$ ) (Figure 3A).

## Effects of silencing p27RF-Rho expression on A549 cells

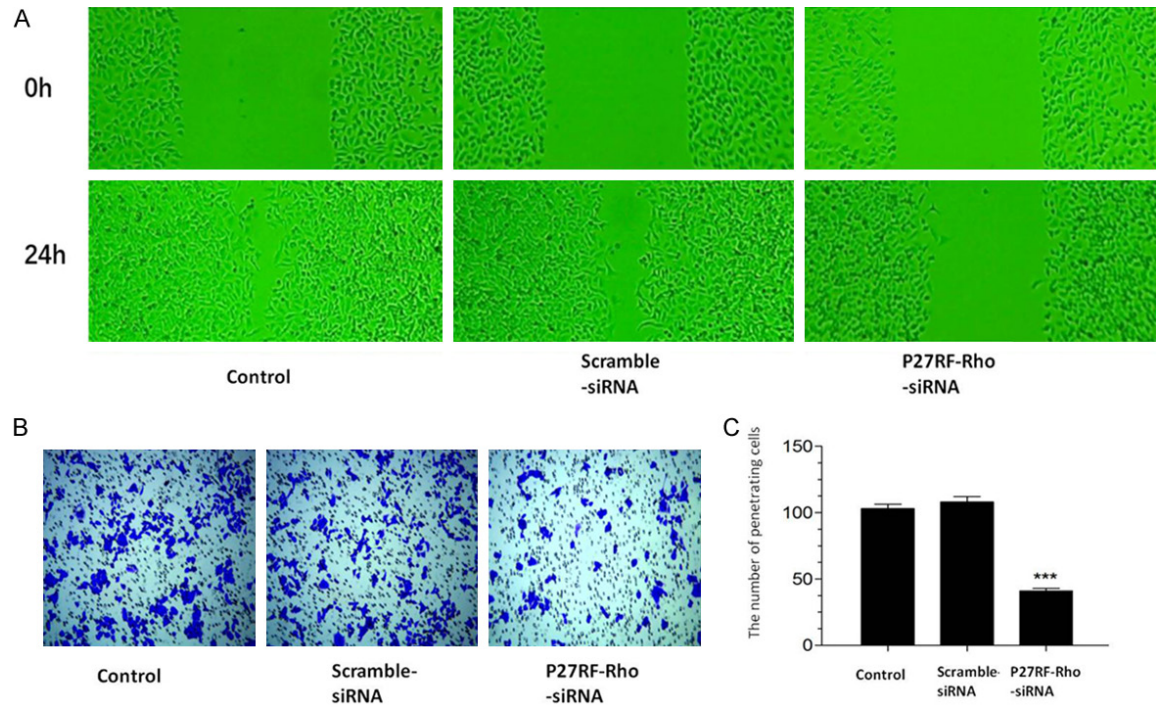


**Figure 3.** A549 cell migration and invasive ability in different groups. Silencing of p27RF-Rho significantly inhibited A549 cell migration (A) and A549 cell invasion (B). The number of penetrating cells in the p27RF-Rho group was decreased compared with the scrambled siRNA negative control group and the control group (C).

### *Silencing p27RF-Rho inhibits A549 cell invasion*

Transwell assays were used to measure the invasive ability of cells in the three groups. The number of penetrating cells in the p27RF-Rho group was  $41 \pm 3.4$ , compared to  $108 \pm 7.2$  in the scrambled siRNA negative control group and  $103 \pm 5.9$  in the blank control group and the difference was statistically significant ( $P < 0.05$ ) (Figure 3B and 3C).

### Discussion

NSCLC is the most prevalent form of lung cancer, accounting for 80-85% of all LC cases. The incidence and mortality rates are high, relapse is common, and prognosis is poor after surgery [20]. At present, the 5-year survival rate of patients with NSCLC is <15%. Although new treatment methods have been developed in recent years, treatment of NSCLC has not significantly improved [21]. Tumor cell invasion and metastasis are the most challenging problems for the treatment of LC. Therefore, it is critical to find new treatments to inhibit these processes. p27RF-Rho is an oncogene that is

widely found in human tumor cells. Silencing of p27RF-Rho can inhibit the growth, differentiation, metastasis, invasion, and apoptosis of tumor cells. Therefore, p27RF-Rho may be a novel target for gene therapy in cancer. Studies have shown that p27RF-Rho can bind to p27<sup>kip1</sup> to regulate the Rho signaling pathway and affect the biological behavior of tumor cells [13]. The function of p27RF-Rho was further verified in the current study.

In this study, a variety of methods were used to detect the expression of p27RF-Rho and measure NSCLC cell proliferation, cell cycle, apoptosis, invasion, and metastasis. A549 NSCLC cells were infected with lentivirus and Western blotting was used to determine the silencing efficiency. The protein levels of p27RF-Rho were significantly higher in the negative control and blank control groups compared to the experimental group. Therefore, the lentiviral construct successfully silenced p27RF-Rho with an efficiency of  $79.8 \pm 2.37\%$ . Cell proliferation was assessed using MTT assays after 12 h of culture. The viability of cells in the p27RF-Rho interference group was significantly lower than that in the negative control and blank con-

## Effects of silencing p27RF-Rho expression on A549 cells

control groups ( $P < 0.05$ ). Therefore, siRNA infection inhibited cell proliferation.

Western blotting and qPCR were used to detect the expression of cell cycle-related proteins and genes. The levels of p16 mRNA and p27<sup>kip1</sup> protein were significantly increased in p27RF-Rho-silenced A549 cells, whereas the levels of CDK5 mRNA and cyclin E protein were significantly decreased. p16 is a key cell cycle regulator, which can inhibit the activity of CDK4 kinase and prevent cells from transitioning from the G1 into S phase, ultimately leading to cell proliferation [22]. p16 is downregulated or absent in a variety of tumors including NSCLC, and functions as a tumor suppressor that affects tumor growth [23]. CDK5 is overexpressed in a variety of malignant tumors including NSCLC, and promotes cell proliferation and abnormal cell apoptosis that are involved in tumor development [24]. Cyclin E is also a key regulator of the cell cycle that mainly functions in the G1 phase. Low levels of cyclin E can arrest cells in the G1 phase and prevent further cell division, which can inhibit cell proliferation and tumor development [25]. However, its overexpression in a variety of malignant tumors affects proliferation of tumor cells [26]. These results suggest that p27RF-Rho may affect proliferation of NSCLC cells by regulating the expression of several cell cycle-related proteins.

p53 is the most important tumor suppressor gene in the body. It regulates multiple signaling pathways and promotes tumor cell apoptosis. It is generally believed that deletion or mutation of p53 is an important contributor to the occurrence of tumors, and that most tumors have p53 deletions or mutations. The apoptosis-related proteins Bcl-2 and Bax are important regulators of apoptosis and cell death [27]. Bcl-2 is an anti-apoptotic protein that is located in the mitochondria, whereas Bax is a pro-apoptotic protein that is mainly located in the cytoplasm. Bcl-2 and Bax form a dimer and upon stimulation, the dimer depolymerizes to cause release of Bcl-2, an increase in the Bcl-2: Bax ratio, and an increase in apoptosis resistance [28]. In this study, Western blotting showed that expression of p53 and Bax in A549 cells was significantly increased after p27RF-Rho was silenced, whereas expression of the antiapoptotic protein Bcl-2 was significantly decreased. These results suggest that

p27RF-Rho can regulate the expression of a variety of apoptotic proteins, thereby affecting NSCLC cell apoptosis. The current study also assessed the migration and invasion of A549 cells using scratch wound and Transwell assays, respectively, and found that these processes were significantly decreased by silencing p27RF-Rho. Together, these data show that p27RF-Rho silencing significantly inhibited NSCLC cell proliferation, invasion, metastasis, and cell cycle progression, and promoted cell apoptosis. The significant differences compared to the negative control and blank control groups indicate that this inhibition is caused by the specific downregulation of p27RF-Rho rather than by the viral vector.

In conclusion, we used RNAi to silence the expression of p27RF-Rho in NSCLC cells and measured cell proliferation, the cell cycle, apoptosis, invasion, and metastasis to explore the potential role of p27RF-Rho for the treatment of NSCLC. The results show that p27RF-Rho RNAi can inhibit expression of p27RF-Rho and inhibit tumor development. Therefore, p27RF-Rho could be considered a potential new target for the treatment of NSCLC. However, tumor development might involve multiple genes. In addition, each cancer gene that promotes tumor development requires a complex signaling system. Therefore, we believe that more mature RNAi technology should be used with the development of precision medical techniques.

### Disclosure of conflict of interest

None.

**Address correspondence to:** Youbin Cui, Department of Thoracic Surgery, The First Hospital of Jilin University, 71 Xinmin Street, Changchun 130021, China. E-mail: cuiyb@jlu.edu.cn

### References

- [1] Wang SS, Zimmermann M, Zhang H, Lin TY, Malfatti M, Haack K, Turteltaub KW, Cimino GD, de Vere White R, Pan CX and Henderson PT. A diagnostic microdosing approach to investigate platinum sensitivity in non-small cell lung cancer. *Int J Cancer* 2017; 141: 604-613.
- [2] Sabari JK, Santini FC, Schram AM, Bergagnini I, Chen R, Mrad C, Lai WV, Arbour KC and Drilon A. The activity, safety, and evolving role of brigatinib in patients with ALK-rearranged non-

## Effects of silencing p27RF-Rho expression on A549 cells

- small cell lung cancers. *Onco Targets Ther* 2017; 10: 1983-1992.
- [3] Dahele M and Damhuis R. The relationship between histology, stage, and type of treatment in patients with early-stage lung cancer. *J Thorac Oncol* 2017; 12: e58-e59.
- [4] Ricciuti B, Metro G, Baglivo S, Colabrese D, Chiari R, Bennati C and Paglialunga L. Long-lasting response to nivolumab and immune-related adverse events in a nonsquamous metastatic non-small cell lung cancer patient. *J Thorac Oncol* 2017; 12: e51-e55.
- [5] Ettinger DS, Akerley W, Borghaei H, Chang AC, Cheney RT, Chirieac LR, D'Amico TA, Demmy TL, Ganti AK, Govindan R, Grannis FW Jr, Horn L, Jahan TM, Jahanzeb M, Kessinger A, Komaki R, Kong FM, Kris MG, Krug LM, Lennes IT, Loo BW Jr, Martins R, O'Malley J, Osarogjagbon RU, Otterson GA, Patel JD, Pinder-Schenck MC, Pisters KM, Reckamp K, Riely GJ, Rohren E, Swanson SJ, Wood DE, Yang SC, Hughes M, Gregory KM; NCCN (National Comprehensive Cancer Network). Non-small cell lung cancer. *J Natl Compr Canc Netw* 2012; 10: 1236-1271.
- [6] Parkin DM, Bray F, Ferlay J and Pisani P. Global cancer statistics, 2002. *CA Cancer J Clin* 2005; 55: 74-108.
- [7] Sangha R, Price J and Butts CA. Adjuvant therapy in non-small cell lung cancer: current and future directions. *Oncologist* 2010; 15: 862-872.
- [8] Raso MG and Wistuba II. Molecular pathogenesis of early-stage non-small cell lung cancer and a proposal for tissue banking to facilitate identification of new biomarkers. *J Thorac Oncol* 2007; 2: S128-135.
- [9] Sharma S, Santiskulvong C, Rao J, Gimzewski JK and Dorigo O. The role of Rho GTPase in cell stiffness and cisplatin resistance in ovarian cancer cells. *Integr Biol (Camb)* 2014; 6: 611-617.
- [10] Porter AP, Papaioannou A and Malliri A. Deregulation of Rho GTPases in cancer. *Small GTPases* 2016; 7: 123-138.
- [11] Suzuki JI, Roy BC, Ogaeri T, Kakinuma N and Kiyama R. Depletion of tumor suppressor Kank1 induces centrosomal amplification via hyperactivation of RhoA. *Exp Cell Res* 2017; 353: 79-87.
- [12] Lu X, Guo H, Chen X, Xiao J, Zou Y, Wang W and Chen Q. Effect of RhoC on the epithelial-mesenchymal transition process induced by TGF-beta1 in lung adenocarcinoma cells. *Oncol Rep* 2016; 36: 3105-3112.
- [13] Hoshino D, Koshikawa N and Seiki M. A p27(kip1)-binding protein, p27RF-Rho, promotes cancer metastasis via activation of RhoA and RhoC. *J Biol Chem* 2011; 286: 3139-3148.
- [14] Xie S, Wang G, Chen G, Zhu M and Lv G. Lentivirus-mediated knockdown of P27RF-Rho inhibits hepatocellular carcinoma cell growth. *Contemp Oncol (Pozn)* 2017; 21: 35-41.
- [15] Sion-Vardy N, Freedman J, Lazarov I, Bolotin A and Ariad S. p27kip1 expression in non-small cell lung cancer is not an independent prognostic factor. *Anticancer Res* 2010; 30: 3699-3704.
- [16] Kruck S, Merseburger AS, Hennenlotter J, Scharpf M, Eyrich C, Amend B, Sievert KD, Stenzl A and Bedke J. High cytoplasmic expression of p27(Kip1) is associated with a worse cancer-specific survival in clear cell renal cell carcinoma. *BJU Int* 2012; 109: 1565-1570.
- [17] Mueller AK, Hammerschmidt-Kamper C and Kaiser A. RNAi in plasmodium. *Curr Pharm Des* 2014; 20: 278-283.
- [18] Berois M, Romero-Severson J and Severson DW. RNAi knock-downs support roles for the mucin-like (AelMUC1) gene and short-chain dehydrogenase/reductase (SDR) gene in *Aedes aegypti* susceptibility to *Plasmodium gallinaceum*. *Med Vet Entomol* 2012; 26: 112-115.
- [19] McRobert L and McConkey GA. RNA interference (RNAi) inhibits growth of plasmodium falciparum. *Mol Biochem Parasitol* 2002; 119: 273-278.
- [20] Barnes H, See K, Barnett S and Manser R. Surgery for limited-stage small-cell lung cancer. *Cochrane Database Syst Rev* 2017; 4: CD011917.
- [21] Yoshioka H, Katakami N, Okamoto H, Iwamoto Y, Seto T, Takahashi T, Sunaga N, Kudoh S, Chikamori K, Harada M, Tanaka H, Saito H, Saka H, Takeda K, Nogami N, Masuda N, Harada T, Kitagawa H, Horio H, Yamanaka T, Fukuoka M, Yamamoto N and Nakagawa K. A randomized, open-label, phase III trial comparing amrubicin versus docetaxel in patients with previously treated non-small-cell lung cancer. *Ann Oncol* 2017; 28: 285-291.
- [22] Fei HJ, Zu LD, Wu J, Jiang XS, Wang JL, Chin YE and Fu GH. PCAF acts as a gastric cancer suppressor through a novel PCAF-p16-CDK4 axis. *Am J Cancer Res* 2016; 6: 2772-2786.
- [23] Chen JL, Chen JR, Huang FF, Tao GH, Zhou F and Tao YJ. Analysis of p16 gene mutations and their expression using exhaled breath condensate in non-small-cell lung cancer. *Oncol Lett* 2015; 10: 1477-1480.
- [24] Wei K, Ye Z, Li Z, Dang Y, Chen X, Huang N, Bao C, Gan T, Yang L and Chen G. An immunohistochemical study of cyclin-dependent kinase 5 (CDK5) expression in non-small cell lung cancer (NSCLC) and small cell lung cancer (SCLC): a possible prognostic biomarker. *World J Surg Oncol* 2016; 14: 34.

## Effects of silencing p27RF-Rho expression on A549 cells

- [25] Wang X, Qi X, Ming X, Wang L, Wang Y and Zhao X. Prognostic value of cyclin E expression in patients with ovarian cancer: a meta-analysis. *J BUON* 2017; 22: 64-71.
- [26] Huang LN, Wang DS, Chen YQ, Li W, Hu FD, Gong BL, Zhao CL and Jia W. Meta-analysis for cyclin E in lung cancer survival. *Clin Chim Acta* 2012; 413: 663-668.
- [27] Malla R, Gopinath S, Alapati K, Gondi CS, Gujrati M, Dinh DH, Mohanam S and Rao JS. Downregulation of uPAR and cathepsin B induces apoptosis via regulation of Bcl-2 and Bax and inhibition of the PI3K/Akt pathway in gliomas. *PLoS One* 2010; 5: e13731.
- [28] Liu G, Wang T, Wang T, Song J and Zhou Z. Effects of apoptosis-related proteins caspase-3, Bax and Bcl-2 on cerebral ischemia rats. *Biomed Rep* 2013; 1: 861-867.